Electron Impact Ionization in the Presence of a Laser Field: A Kinematically Complete ($n\gamma e$,2e) Experiment

C. Höhr, A. Dorn, B. Najjari, D. Fischer, C. D. Schröter, and J. Ullrich
Max-Planck-Institut für Kernphysik, Saupfercheckweg 1, D-69117 Heidelberg, Germany
(Received 30 July 2004; published 21 April 2005)

Single ionization of He by 1 keV electron impact in the presence of an intense ($I = 4 \times 10^{12}$ W/cm^2) laser field ($\lambda = 1064$ nm) has been explored in a kinematically complete experiment using a reaction microscope. Distinct differences in the singly to fully differential cross sections compared to the field-free situation are observed which cannot be explained by a first-order quantum calculation. Major features, such as the number of photons exchanged and the modification of the energy spectrum of emitted electrons, can be understood qualitatively within a simple classical model.

DOI: 10.1103/PhysRevLett.94.153201 PACS numbers: 34.80.Qb, 32.80.Fb, 32.80.Rm, 34.80.Dp

The investigation of collisions in the presence of a strong electromagnetic field was first addressed theoretically more than half a century ago, when cross sections for ''multiquantum bremsstrahlung and absorption'' were derived for the case of elastic scattering (see, e.g., [1]). The topic has attracted continuous and increasing attention over the years (see, e.g., [2] for a review) culminating in a series of recent theoretical papers where the motivation was several-fold. First, field-assisted electron impact excitation and ionization have now been demonstrated to be the basic underlying mechanisms for nonsequential, multiple ionization in strong laser fields [3–5]. Here, a tunneled electron, driven by the field, recollides with its parent ion (for a review see [6]) thereby enhancing the multiple ionization yields by several orders of magnitude compared to uncorrelated, sequential tunneling processes. Despite its paramount importance, the dynamics of the field-assisted electron recollision (i.e., the momentum exchange between the two active electrons, which strongly differ from the field-free behavior) are far from understood. Laser-assisted (e, 2e) data under well-controlled experimental conditions could help in understanding this process. Second, an intense laser field was shown to considerably modify subfemtosecond electron transfer processes in slow ion-atom collisions [7], supporting hopes for ultrafast electronic quantum control with possible applications in laser-driven fusion, plasma heating, or the development and understanding of ultrafast optoelectronic devices. Third, the dynamical situation *per se* is most appealing from a fundamental point of view. For example, it has been predicted that thousands of low-energy photons might be exchanged with even a quite weak laser field during hard collisions of a fast ion with a target electron, illustrating the extremely effective coupling between the radiation field and collision-accelerated charged particles [8].

Experimentally, multiphoton emission and absorption occurring during *elastic* electron-atom collisions in the presence of a CO_2 laser field were first demonstrated in 1977 [9] and found to be in qualitative agreement with theoretical models based on the soft-photon ''Kroll-Watson approximation'' (KWA) [10]. In this model, the laser projectile interaction is treated to all orders, while the laser target interaction is neglected. Severe (order-of-magnitude) discrepancies to the KWA prediction found more recently [11] under certain geometrical conditions have initiated a series of sophisticated treatments using the impulse approximation, a full Floquet [12] or a coupled-channel approach [13]. Only the last of these found a qualitative confirmation of the experimentally observed slow variation of the cross sections with the number of exchanged photons, still differing by more than 2 orders of magnitude on an absolute scale.

In 1987, simultaneous electron-photon excitation of helium was experimentally observed for the first time [14] in *inelastic* laser-assisted electron-atom collisions, which had been already theoretically addressed (e.g., [15]). More recently, an experiment was performed at higher laser frequencies [16] and theory developed beyond a perturbative treatment [17–19].

In this Letter, we report on the first realization of an electron impact *ionization* experiment in the presence of a strong laser field, where the momenta of both outgoing electrons are determined, allowing investigation of their respective emission characteristics. Using multiparticle imaging techniques (reaction microscopes [20]) under laser on-off conditions but otherwise exactly identical experimental conditions, we clearly demonstrate significant deviations of singly up to fully differential cross sections caused by the exchange of up to approximately 10 photons from a Nd-doped yttrium aluminum garnet (Nd:YAG) laser field. The experimental results are compared to the predictions of a first-order Born-approximation (FBA) calculation and clear deviations are observed.

The experiment was performed at the Max-Planck-Institut für Kernphysik by overlapping a 1 keV pulsed electron beam (20 Hz, 1 ns) and a Nd:YAG laser beam (10 Hz, 7 ns, 1064 nm, 3 J) at the position of a supersonic helium target beam (1 mm diameter, 10^{12} atoms/cm^3) at a base pressure of 10^{-8} Torr (Fig. 1). Care was taken that the electron beam with a diameter of 140 μm was completely

embedded in both space and time within the laser pulse which had a non-Gaussian, approximately flat intensity distribution over a diameter of 100 μm (intensity: $I = 4 \times 10^{12}$ W/cm^2). The projectile pulses which have a time separation of 50 ms were fired alternately with and without the laser, and therefore field-free $(e, 2e)$ cross sections were measured under exactly identical experimental conditions.

In the reaction microscope, the low-energy emitted He electron "b" (exchange with the projectile electron "a" can safely be neglected at high energies) and the recoiling He^+ target ion "R" are projected by homogeneous electric (2.5 V/cm) and magnetic (9.7 Gauss) fields upon position- and time-sensitive microchannel plate detectors. The ion and electron longitudinal momentum components ($k_\parallel = k_z$) (along the z axis in Fig. 1) are deduced from the times of flight (TOFs), respectively. The two respective transverse momentum components [k_x, k_y, with $k_\perp = (k_x^2 + k_y^2)^{1/2}$] are obtained from the impact positions on the detectors in the xy plane and the TOFs (for details see [20,21]). Thus, measuring the momentum vectors of both target fragments ($\vec{k}_b$, $\vec{k}_R$) in coincidence in a kinematically complete experiment allows one to deduce the momentum of the scattered electron $\vec{k}'_a = \vec{k}_a - \vec{k}_b - \vec{k}_R$ ($\vec{k}_a$: projectile electron initial mometum) as well as the momentum transfer $\vec{q} = \vec{k}_a - \vec{k}'_a = \vec{k}_b + \vec{k}_R$ occurring during the collision with $\vec{q} = (q_\parallel, \vec{q}_\perp)$. Under present conditions, all target electrons with longitudinal momenta of $k_{b\parallel} > -1.4$ a.u. ($-z$ direction) and transverse momenta of $k_{b\perp} < 1.1$ a.u. are recorded simultaneously with resolutions $\Delta k_{b\parallel}, \Delta k_{b\perp} < 0.08$ a.u. (atomic units, a.u., are used throughout with $e = m = \hbar = 1$; e, m, electron charge and mass; $\hbar$, Planck's constant). The transverse electron momentum resolution depends on the TOF, and the given value is an average. The He^+ ion acceptance was $k_{R\parallel} < 116$ a.u. and $k_{R\perp} < 4$ a.u. with resolutions along the various coordinates of $\Delta k_{R\parallel} < 0.12$ a.u., $\Delta k_{Rx} < 0.13$ a.u., and $\Delta k_{Ry} < 0.25$ a.u., the last of these being limited by the inherent 0.83 K temperature of the supersonic jet along the direction of expansion.

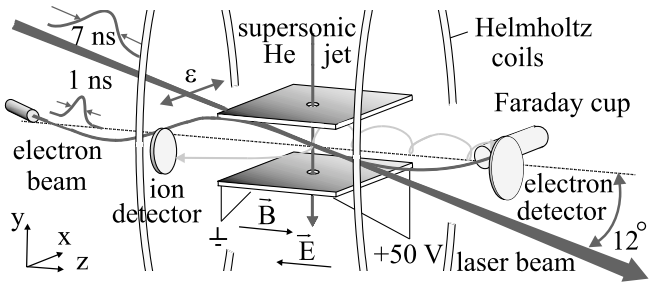

FIG. 1. Reaction microscope: The electron beam hits the target after a full-turn cyclotron cycle before propagating to the off-axis Faraday cup. The laser beam overlaps the electron beam collinearly in the interaction volume.

Two different laser-induced reactions were observed. First, the electron beam might excite the helium target to various states in a primary step: $e^- + \mathrm{He} \rightarrow e^- + \mathrm{He}^*$. These are then transferred to the continuum by absorption of one or more photons from the laser in a second step: $\mathrm{He}^* + n\gamma \rightarrow \mathrm{He}^+ + e^-$. The absorption of up to $n = 3$ photons ($\omega = 0.043$ a.u. $\hat{=} 1.17$ eV) from the different Stark-shifted excited states ($1snp$), leads to an increased yield of low-energy electrons with $E_b < 0.11$ a.u. ($\hat{=} 3$ eV), beyond which no significant contribution could be observed. This electron impact excitation photoabsorption ionization reaction is very interesting by itself and will be investigated in a subsequent paper. Second, the direct $(e, 2e)$ ionization reaction modified by the simultaneous absorption or emission of n photons, i.e., the $(n\gamma e, 2e)$ process, and the subject of this Letter, is observed:

$$1\ \mathrm{keV}\ e^- + \mathrm{He} \pm n\gamma \rightarrow 2e^- + \mathrm{He}^+.$$

In order to discriminate from the first reaction, all of the following spectra are recorded under the condition that the slow electron energy $E_b > 0.11$ a.u.

In principle, the number of exchanged photons can be determined in our kinematically complete experiment from the measured momenta of all target fragments, yielding the total inelasticity Q' of the reaction $Q'/v = (Q \pm n\hbar\omega)/v = k_{R\parallel} + k_{b\parallel} - E_b/v$ (v, projectile velocity; Q, change of the total internal energy of the target). For single ionization without photon exchange ($n = 0$), this is just the ionization potential $Q' = Q = IP = 0.904$ a.u. $= 24.59$ eV. Because of the jet-temperature limited recoiling ion momentum resolution and the large projectile velocity of 8.57 a.u., the overall Q'-value resolution is restricted to about 1.1 a.u., which is not sufficient for the discrimination of single photon exchanges with $\Delta Q' = 0.043$ a.u. Nevertheless, distinct information on the number of exchanged photons "n" as well as on their probability distribution can be extracted from the present experiment.

In Fig. 2, experimental and theoretical cuts through the doubly differential electron emission spectra $d^2\sigma/dq_\perp dE_b$ [Fig. 2(a)] are shown along with differences of such spectra for laser on-off conditions, i.e., field-assisted (FA) and field-free (FF) conditions for different transverse momentum transfers $q_\perp = |\vec{q}_\perp|$ by the scattered electron [Figs. 2(b)–2(d)]. Whereas nearly no effect due to the presence of the laser can be observed in the electron spectra alone [Fig. 2(a)], distinct patterns are found in the experimental as well as the theoretical difference spectra. At low momentum transfers [Fig. 2(b)] an oscillatory behavior of the experimental difference occurs which becomes less pronounced with increasing $q_\perp$, merging into only a slight enhancement of the laser-assisted cross section for low-energy electron emission [0.11 a.u. (3 eV) $< E_b < 0.55$ a.u. (15 eV)] at the largest $q_\perp$ in Fig. 2(d). Within the experimental error bars, rough agreement between experimental results and theoretical predictions is found at large momentum transfers, whereas distinct dif-

ferences occur for smaller $q_\perp$. This is in qualitative agreement with recent findings for elastic scattering in the presence of a laser field where deviations between experiment and theories were observed for small scattering angles of the projectile electron, i.e., for small momentum transfers [11–13].

Within the present theoretical model, described in detail in a forthcoming paper, the interaction of the projectile with the laser field is treated exactly to all orders by using an incoming and outgoing electron Volkov state. The projectile-target interaction is taken into account within the FBA, in the sense that the interaction of the projectile and the target is described via the exchange of one virtual photon, which is sufficient for a projectile velocity of 8.57 a.u. The final state neglects the electron-electron as well as the projectile-He^+ interactions. The slow emitted electron is described by a Coulomb-Volkov state. This includes the interaction of the slow electron with the residual ion and also with the laser field. Moreover, the initial target state is taken to be unperturbed by the laser field, i.e., so-called dressing is not accounted for.

We have tried to explain our results and extract the number distribution of exchanged photons by a simple classical consideration. An electron emitted into the continuum of a classical electric field oscillating with a frequency of ω will gain additional energy depending on its initial emission energy E_b^i, its ponderomotive potential (i.e., its mean quiver energy in the oscillating field $U_P = 2\pi I/c\omega^2$ with $I = 6.2 \times 10^{-4}$ a.u. the intensity of the laser field and c the velocity of light), and the phase ωt_0 in the field when it was ejected in the collision. The final energy E_b for an angle θ between the momentum vector $\vec{k}_b$ and the polarization of the field is $E_b \approx E_b^i - \sqrt{8E_bU_P}\sin(\omega t_0)\cos\theta + 2U_P\sin^2(\omega t_0)$. If the electron is fast enough and leaves the laser focus within a time shorter than the laser pulse duration (which is the case for all energies considered here), it is accelerated by the ponderomotive potential gradient and gains the additional kinetic energy U_P. In this model, the energy exchanged between the laser field and the projectile is neglected. On the basis of the Kroll-Watson model, this is justified for small projectile scattering angles which dominate for single ionization [Fig. 2(b)]. The maximum number of exchanged photons would then simply be $n^{\max} = \pm(E_b - E_b^i)/\hbar\omega$. Averaging over all n, taking the measured FF-emitted electron energy distribution and folding it with a field-induced broadening due to photon exchange yields a modified electron spectrum. The difference between this spectrum and the FF energy distribution [solid line in Fig. 2(b)] is found to be in the best agreement with the measured value for an assumed laser intensity of 5.44×10^{-4} a.u.$\hat{=}3.5 \times 10^{12}$ W/cm^2, slightly lower than the experimentally determined result but well within the error bars. Moreover, the distribution of the number n of exchanged photons obtained with this simple model is considerably broader than the one calculated within the FBA. This is illustrated in Fig. 3(a), where the ratio of the classical model to the FBA photon distribution is shown. The broadening is again in accordance with the previously mentioned elastic scattering results for small scattering angles, where the experimental photon number distribution is much broader than predicted.

As described before, one can obtain direct information on the number n of exchanged photons by examining the Q' value of the reaction. Subtracting the experimental FF Q-value distribution from the FA one [Fig. 3(b)] shows an oscillatory behavior resulting from a distinct broadening of the FA spectrum (data points). Taking the photon number distribution extracted from our simple model discussed above, a FA Q-value spectrum can be simulated by folding this number distribution with the FF Q-value spectrum. Subtracting the FF spectrum from the result yields the full

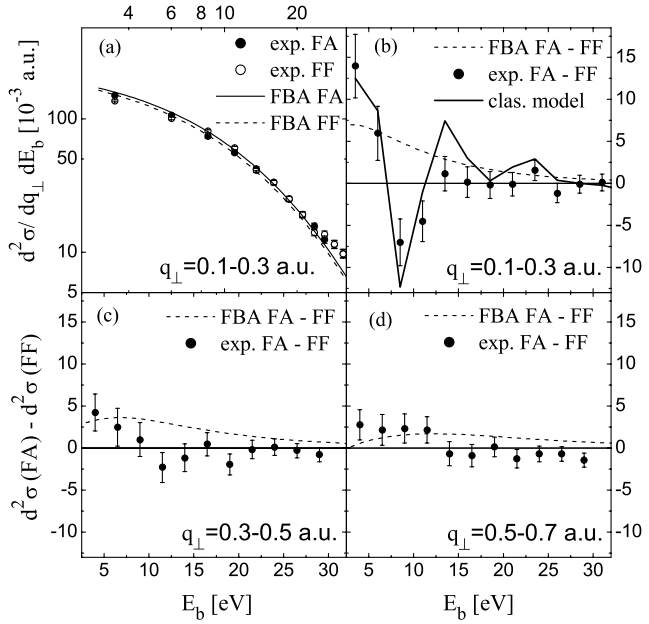

FIG. 2. Cuts through the doubly differential cross sections $d^2\sigma/dq_\perp dE_b$ as a function of the electron energy E_b for different transverse momentum transfers $q_\perp$. (b)–(d) Difference field-assisted (FA) minus field-free (FF) doubly differential cross section. The experimental data in (a) are scaled by a common factor to fit the overall size of the theory.

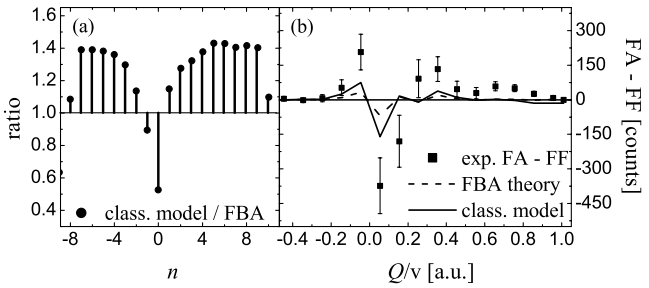

FIG. 3. (a) Ratio of the classical model-FBA photon distributions (b) difference FA-FF Q-value spectra for $q_\perp < 0.5$ a.u.

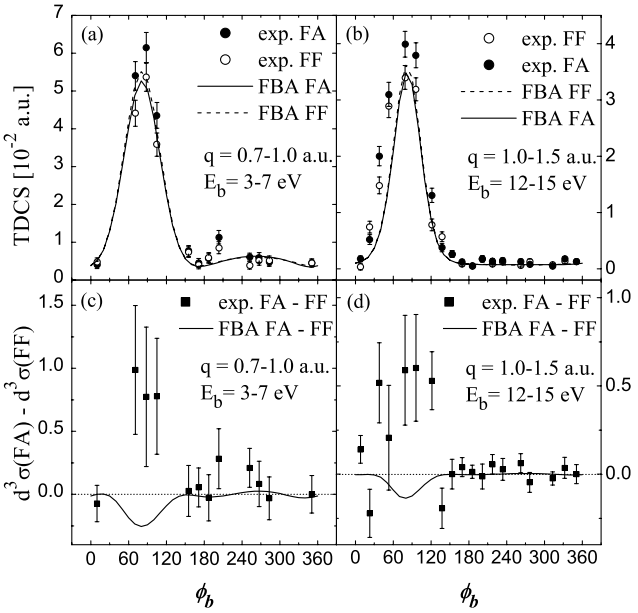

FIG. 4. Cuts through the triply differential cross sections (TDCS) as a function of the emission angle ϕ_b of the ejected electron in the scattering plane with an opening angle of $\pm 20°$.

line in Fig. 3(b) and is in reasonably good agreement with the data. Instead, taking the number distribution of exchanged photons from our FBA calculation yields a considerably worse agreement [broken line in Fig. 3(b)], demonstrating again the enhanced probability of exchanging larger numbers of photons.

Finally, we present cuts through the triply differential cross sections TDCS $= d^3\sigma/2\pi k_b d\Omega_b dE_b dq_\perp$ in Fig. 4 in the so-called coplanar geometry (the target electron is emitted into the scattering plane) for different momentum transfers q and emitted electron energies as indicated in the figure. For FA as well as FF conditions, one finds a distinct maximum along the momentum transfer direction, called the "binary peak," pointing mainly towards 90°, representing target electrons being emitted as a result of a binary collision with the projectile. For all emission energies and momentum transfers, the measured data are in fair agreement with the prediction of the FBA as expected for large projectile energies.

Deviations between FA and FF cross sections are observed in the difference FA − FF in Figs. 4(c) and 4(d). Surprisingly (and in disagreement with early calculations [22] as well as with the present predictions), the binary peak is enhanced under most of the explored dynamical conditions. Whereas the magnitude of the effect seems to be reasonably described by the calculations, the effect itself, i.e., enhancement or diminution of the peak, seems to be reversed. It would be interesting to compare our experimental data with the results of more refined, nonperturbative calculations that take target polarization or dressing of the initial state into account [23–27].

In summary, we have presented the first experimental laser-assisted kinematically complete $(n\gamma e, 2e)$ measurements and have compared them with the results of an FBA calculation. Distinct differences in doubly to triply differential cross sections between laser on-off conditions are observed which are poorly described by the first-order theory. A simple classical consideration to estimate the number distribution of exchanged photons shows this distribution to be considerably broader than predicted. This finding is in qualitative agreement with recent experimental results of field-assisted elastic scattering at small momentum transfers as well as with calculations going beyond a first-order treatment.

In the future, we expect considerably enhanced resolution at lower electron impact energies such that different channels due to different numbers of exchanged photons will become distinguishable. Such data will be of indispensable importance for the understanding of the recollision dynamics in strong-field nonsequential double ionization and will certainly challenge theory.

We acknowledge support by the Leibniz-Programm of the Deutsche Forschungsgemeinschaft, from the MPG and the GSI. We thank A. Voitkiv for fruitful discussions.

[1] F. V. Bunkin and M. V. Fedorov, Sov. Phys. JETP **22**, 844 (1966), and references therein.
[2] F. Ehlotzky *et al.*, Phys. Rep. **297**, 63 (1998).
[3] Th. Weber *et al.*, Phys. Rev. Lett. **84**, 443 (2000).
[4] R. Moshammer *et al.*, Phys. Rev. Lett. **84**, 447 (2000).
[5] A. Rudenko *et al.*, Phys. Rev. Lett. **93**, 253001 (2004).
[6] R. Dörner *et al.*, Adv. At. Mol. Opt. Phys. **48**, 1 (2002).
[7] T. Kirchner, Phys. Rev. A **69**, 063412 (2004).
[8] A. B. Voitkiv and J. Ullrich, J. Phys. B **34**, 1673 (2001).
[9] A. Weingartshofer *et al.*, Phys. Rev. Lett. **39**, 269 (1977).
[10] N. M. Kroll and K. M. Watson, Phys. Rev. A **8**, 804 (1973).
[11] B. Wallbank and J. K. Holmes, Phys. Rev. A **48**, R2515 (1993); Can. J. Phys. **79**, 1237 (2001).
[12] L. W. Garland *et al.*, J. Phys. B **35**, 2861 (2002).
[13] S. Geltman, J. Phys. B **35**, 4787 (2002).
[14] N. J. Mason and W. R. Newell, J. Phys. B **20**, L323 (1987).
[15] N. K. Rahman and F. H. M. Faisal, J. Phys. B **9**, L275 (1976).
[16] S. Luan *et al.*, J. Phys. B **24**, 3241 (1991).
[17] A. Makhoute *et al.*, J. Phys. B **35**, 957 (2002).
[18] S. Vučić, Phys. Rev. A **51**, 4754 (1995).
[19] P. Francken and C. J. Joachain, Phys. Rev. A **41**, 3770 (1990).
[20] J. Ullrich, Rep. Prog. Phys. **66**, 1463 (2003).
[21] R. Moshammer *et al.*, Nucl. Instrum. Methods Phys. Res., Sect. B **108**, 425 (1996).
[22] P. Cavaliere *et al.*, Phys. Rev. A **24**, 910 (1981).
[23] C. J. Joachain *et al.*, Phys. Rev. Lett. **61**, 165 (1988).
[24] P. Martin *et al.*, Phys. Rev. A **39**, 6178 (1989).
[25] A. Makhoute *et al.*, J. Phys. B **32**, 3255 (1999).
[26] M. Bouzidi *et al.*, J. Phys. B **34**, 737 (2001).
[27] S-M. Li *et al.*, J. Phys. B **35**, 557 (2002).